DOI: 10.1002/ejic.201100620

Syntheses and Structures of Two Dimethyl Diselenide–Diiodine Adducts and the First Well Characterized Diorgano Disulfide–Nitrosonium Adduct

Birgit Mueller,[a] Teemu T. Takaluoma,[b] Risto S. Laitinen,[b] and Konrad Seppelt*[a]

Keywords: Main group elements / Density functional calculations / Iodine / Chalcogens / Diorgano dichalcogenides / Nitrosonium

The syntheses and crystal structures of two new dimethyl diselenide–iodine adducts are described as well as the synthesis and crystal structure of the first diorgano disulfide–nitrosonium adduct. The reaction of the NO^+ cation with R_2S_2 (R = Me, Et, *neo*-Pent, H, CN, CF_3, 4-pyridyl, 2-Prop, Ph, Ad) has been investigated theoretically with DFT. Charge transfer is the main mechanism for adduct formation. Electron density is transferred from the diorgano disulfide HOMO, which is mainly composed of sulfur lone pairs, to the NO^+ cation LUMO (π^*).

Introduction

Adduct formation of organic molecules containing group16 donor atoms (E = S, Se, Te) have been the subject of renewed activity, not only in the case of reactions with diiodine, but also as nitrosonium complexes. The continuously increasing interest in these species is because of their implications to different fields of research, which span from synthetic to biological, materials and industrial chemistry.[1] Diiodine adducts have biological and pharmaceutical applications.[2] New chalcogen-based materials have important electrical properties.[3,4] The interest in nitrosonium complexes stems from the fact that they are intermediates in a series of reactions[5] and from the discovery of the unique role of the NO molecule in biochemical processes.[6] It is assumed that the nitrosonium cation and some molecules generating the nitrosonium ion are involved in neurotoxic and neuroprotective processes of nitric oxide[7] and participate in DNA cross-linking.[8] Investigations of the structures and reactivities of nitrosonium complexes are essential to the understanding of the role of the NO^+ cation in various chemical reactions ranging from ionospheric[9] to biochemical processes,[7a–7c] which give rise to different classes of organic compounds.[10] Some simple adducts have been reported by du Mont[11]: $[(TIP_2Se_2)_2{\cdot}I_2]$ and $[Ph_2Se_2{\cdot}I_2]$.[12] On this basis, some selenophosphane iodine species have been discovered.[13] In this paper we describe two adducts of dimethyl diselenide and diiodine with different stoichometries, $[Me_2Se_2{\cdot}2I_2]$ and $[Me_2Se_2{\cdot}I_2]$, as well as the structure and bonding situation of the first diorgano disulfide–nitrosonium adduct, $[C_{10}H_{22}S_2{\cdot}NO^+TfO^-]$.

Results and Discussion

Synthesis and X-ray Crystallography

Following our results from the oxidation of diorgano dichalcogenides with nitrosyl triflate, which formed cationic four-membered rings,[14] we used diiodine as an oxidizing reagent. These investigations yielded two new neutral charge transfer (CT) adducts of dimethyl diselenide and diiodine. The first dimethyl diselenide–diiodine adduct, $[Me_2Se_2{\cdot}2I_2]$, was observed as a byproduct in the reaction of dimethyl diselenide, nitrosyl triflate and diiodine in the ratio 3:2:2 (Scheme 1).

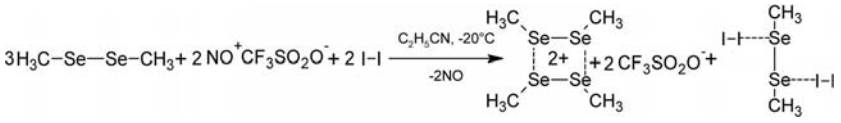

Scheme 1.

By changing the ratio (1:1:1), an adduct with a different stoichiometry was formed, $[Me_2Se_2{\cdot}I_2]$, which is also specifically synthesized by the reaction of dimethyl diselenide with diiodine in the absence of nitrosyl triflate (Scheme 2).

[a] Institut für Chemie und Biochemie – Anorganische Chemie, Freie Universität Berlin,
14195 Berlin, Germany
E-mail: seppelt@chemie.fu-berlin.de
[b] Department of Chemistry,
P. O. Box 3000, 90014 University of Oulu, Finland
E-mail: risto.laitinen@oulu.fi

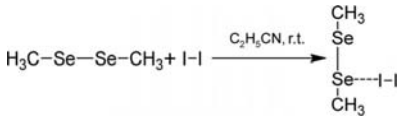

Scheme 2.

$[Me_2Se_2{\cdot}2I_2]$ and $[Me_2Se_2{\cdot}I_2]$ crystallize in the monoclinic space group $P2_1/n$. They show the often described linear E–X–X arrangement of neutral CT "spoke" adducts[1] (Figure 1).

As a result of the coordination of the diiodine to the dimethyl diselenide, the I–I bond is lengthened compared to pure I_2 (see Table 1). The Se–I bond length is 2.93 Å in $[Me_2Se_2{\cdot}I_2]$ and 2.85 Å in $[Me_2Se_2{\cdot}2I_2]$. The Se–I distances are shorter than the sum of the van der Waals radii[15] and in the range of coordinative bonds of other selenium–iodine adducts.[16]

The selenium and the two iodine atoms show a Se–I–I angle of 179° in $[Me_2Se_2{\cdot}I_2]$ and 180° in $[Me_2Se_2{\cdot}2I_2]$. The Se–Se–I angle is larger than 90° in both cases, 93.4° in $[Me_2Se_2{\cdot}I_2]$ and 98.1° in $[Me_2Se_2{\cdot}2I_2]$. The C–Se–Se–C torsion angle in $[Me_2Se_2{\cdot}2I_2]$ changes from the *gauche* conformation of uncoordinated dimethyl diselenide to a *trans* configuration, so that the selenium and iodine atoms are arranged in planes. The angle between the I–Se–Se–I and C–Se–Se–C planes is 81° (Figure 2).

The intermolecular contacts between the iodine molecules are 3.70 Å, which is longer than in pure I_2[18] and shorter than the sum of the van der Waals radii.[15] This results in a step-like arrangement in the crystal. In $[Me_2Se_2{\cdot}I_2]$, the intermolecular iodine contacts lead to a net-like structure that is also observed for molecular iodine,[18] even though the distances between the iodine molecules are longer because of the coordination to the dimethyl diselenide (Figure 3).

All these properties are typical for CT spoke adducts between chalcogen donor molecules and dihalogens, where an average value very close to 180° is generally observed for the E–X–X angle, which indicates a strong directionality at short E–X distances (2.4–3.0 Å) in the formation of chalcogen and dihalogen CT spoke adducts. The reason why the interaction between these molecules results in adducts containing an almost linear E–X–X fragment is, simplistically speaking, transfer of electron density from the nonbonding orbitals of the donor atom into the lowest unoccupied molecular orbital (LUMO) of the dihalogen acceptor molecule. The LUMO is a σ_u^* orbital lying along the mo-

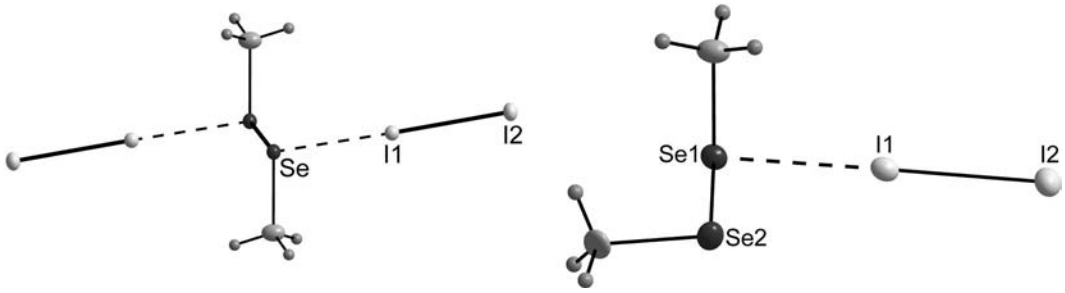

Figure 1. Molecular structures of $[Me_2Se_2{\cdot}2I_2]$ and $[Me_2Se_2{\cdot}I_2]$ with thermal ellipsoids at 50% probability.

Table 1. Comparison of the structural parameters of Me_2Se_2, I_2, $[Me_2Se_2{\cdot}I_2]$ and $[Me_2Se_2{\cdot}2I_2]$.

	Se1–Se2 [Å]	Se–C [Å]	Se–Se–C [Å]	Se–Se–I [Å]	C–Se–Se–C [Å]	I–I [Å]	Se···I [Å]	I···I [Å]
$[Me_2Se_2]$[17]	2.31	1.94, 1.95	101.7, 100.0	–	85	–	–	–
I_2[18]	–	–	–	–	–	2.72	–	3.50
$[Me_2Se_2{\cdot}I_2]$	2.3328(5)	1.9627(4), 1.9475(4)	101.739(5), 99.270(7)	93.355(5)	89.061(8)	2.8057(5)	2.9323(5)	3.8745(7)
$[Me_2Se_2{\cdot}2I_2]$	2.3866(3)	1.9699(3)	94.467(3)	94.467(3)	180.000(6)	2.8524(9)	2.8490(9)	3.6893(10)

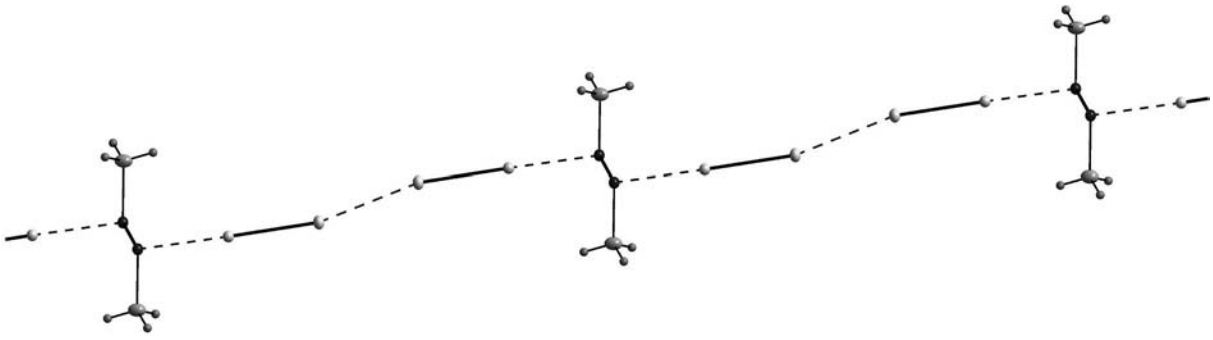

Figure 2. Interactions between the I_2 moieties in the crystal structure of $[Me_2Se_2{\cdot}2I_2]$.

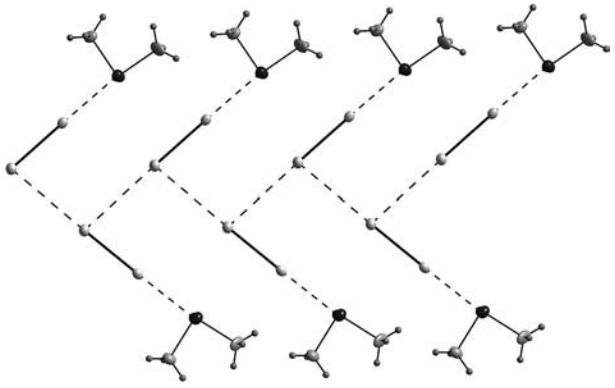

Figure 3. Interactions between the I_2 moieties in the crystal structure of $[Me_2Se_2{\cdot}I_2]$.

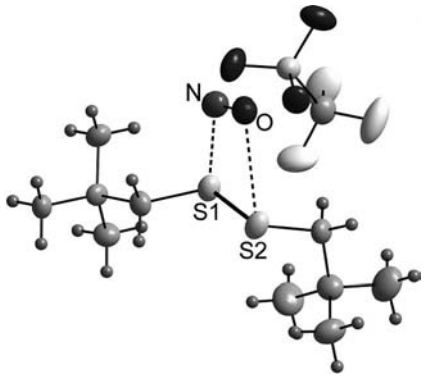

Figure 4. Molecular structure of $[C_{10}H_{22}S_2{\cdot}NO^+TfO^-]$ with thermal ellipsoids at 50% probability.

lecular axis.[1] The increase of the X–X bond length can be finely modulated by using donors of different strength, which means changing either the chalcogen donor, its chemical environment or, as demonstrated here, the stoichiometry.

A general qualitative observation is that upon decreasing the difference in electronegativity between the halogen and the chalcogen, CT spoke adducts are more likely to be formed than "T-shaped" hypervalent adducts. Indeed, the number of structurally characterised T-shaped adducts decreases on passing from chlorine to iodine for S- and Se-containing donor molecules, and hypervalent sulfur compounds with iodine are unknown. On the other hand, no CT di- or interhalogen adducts are known for organic compounds containing tellurium as the donor atom.[1] So it is not surprising that the reaction described in Scheme 1 with diethyl ditelluride yielded the four membered cationic tellurium species[14] and unreacted diiodine rather than any additional organotellurium iodine compound.

In search of a four-membered cation for sulfur analogous to those formed in the case of selenium and tellurium, we tried to oxidize diorgano disulfides with nitrosyl triflate.[14] Under the same reaction conditions no oxidation occurs and, as shown in Scheme 3, an adduct is formed (R = *neo*-pentyl).

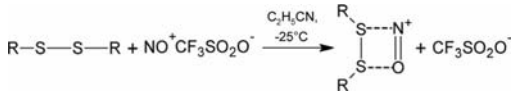

Scheme 3.

The solution is red; however, at –80 °C green crystals grow and the solution turns yellow. The solid-state structure is shown in Figure 4. If the green crystals are redissolved, the solution becomes red again. We interpret this colour change between the solid and dissolved state as follows: due to exchange process in solution where basic solvent molecules are involved, the CT interaction between the di-*neo*-pentyl disulfide and the NO^+ is weakened. Such cases have been described before.[19] A computational simulation of this behaviour is beyond the scope of this work, in particular the calculation of the CT energy in solution.

$[C_{10}H_{22}S_2{\cdot}NO^+TfO^-]$ crystallizes in the monoclinic space group *C2/c*. The known *gauche* configuration of diorgano dichalcogenides[17] changes to a *trans* configuration with a C–S–S–C torsion angle of 160°. The N–O bond length is 1.1 Å, similar to those of other nitrosonium CT complexes.[20] A trapezoid is formed by the S atoms and NO^+ with S–N and S–O bond lengths of 2.3 and 2.9 Å, respectively, which are shorter than the sum of the van der Waals radii.[15] The trapezoid is nearly planar (∠ S–S–O–N 3.7°).

This result shows that the oxidation potential of NO^+ is not high enough to oxidize diorgano disulfides under the given reaction conditions.

The reactions of dimethyl and diethyl disulfides with nitrosonium triflate (Scheme 3) resulted in the formation of coloured solutions. However, no crystals could be isolated from these solutions.

Disulfide Adduct Formation

Theoretical calculations have been used to estimate the stability of the NO^+ adducts of dimethyl, diethyl and di-*neo*-pentyl disulfide. In addition the stability of the hypothetical nitrosonium adducts of the disulfides, R_2S_2, where R = H, CN, CF_3, 4-pyridyl, 2-Prop, Ph and Ad, have been considered for comparison.

The standard Gibbs energy changes of the reaction $R_2S_2 + NO^+ \rightarrow [R_2S_2{-}NO]^+$ has been estimated for the ten disulfides at the M06L/def2-TZVPP level of theory (Table 2).

Table 2. Change in standard Gibbs energy [kJ/mol] for the reaction $R_2S_2 + NO^+ \rightarrow [R_2S_2{-}NO]^+$.

CN	CF_3	4-Pyridyl	H	Ph	2-Prop	Me	Et	*neo*-Pent	Ad
23.8	–3.2	–40.6	–58.4	–65.7	–73.8	–81.8	–86.7	–89.0	–98.3

The formation of the diadamantyl adduct is predicted to be the most favourable. The standard Gibbs energy changes in the formation of four other adducts in which the organic substituent of the disulfide is electron donating (i.e. *neo*-Pent, Et, Me and 2-Prop) are 9.3, 11.6, 16.5 and 24.5 kJ/mol less favourable than that of the adamantyl-substituted

adduct, respectively. The adduct formation in all disulfides with electron-withdrawing substituents is predicted to be quite unfavourable. In fact, the adduct formation between $(CN)_2S_2$ and NO^+ is strongly endergonic. The standard Gibbs energy change for the NO^+ adduct formation with dimethyl, diethyl and di-*neo*-pentyl disulfides all lie within a close energy range, with only 7.2 kJ/mol difference in free energy between dimethyl and di-*neo*-pentyl disulfide. This small energy difference would support the existence of the unobserved adducts of dimethyl and diethyl disulfides, whose preparation was attempted for this contribution. But as mentioned above, the crystalline product could only be isolated in case of the di-*neo*-pentyl disulfide adduct.

M06L/def2-TZVPP optimized geometries of $[R_2S_2–NO]^+$ cations are presented in Table 3 together with those of free R_2S_2, which were computed for comparison. Experimental structures are also shown in Table 3 where available. For all adduct cations, the R–S–S–R torsion angle is significantly larger than that in the free disulfides. The N–O bond has lengthened from the calculated value of 1.059 Å for the free NO^+. Adduct formation also leads to the shortening of the S–S bond, the only exceptions being for dicyano disulfide, dipyridyl disulfide and diphenyl disulfide. The slight increase of electron density value (ρ) in the S–S bond critical point (BCP) upon adduct formation implies an increase in the bond strength and correlates with the shortening of the S–S bond length.

Upon the formation of all adducts, a significant delocalization of the electron density from the disulfide to the nitrosonium cation, carrying a formal charge of +1, can be seen, as shown in Table 4.

Table 4. Partial charges (AIM) for three partitions of the adduct: two sulfur atoms (S^x), organic groups (R^x) and the nitrosonium cation.

	S^1	S^2	R^1	R^2	N	O	N–O
CN	+0.658	+0.633	–0.446	–0.471	+0.942	–0.316	+0.626
CF_3	+0.191	+0.159	+0.054	+0.025	+0.895	–0.325	+0.570
4-Pyridyl	+0.213	+0.158	+0.112	+0.085	+0.778	–0.345	+0.433
H	+0.274	+0.219	+0.050	+0.029	+0.778	–0.351	+0.428
Ph	+0.208	+0.115	+0.180	+0.151	+0.708	–0.363	+0.345
2-Prop	+0.152	+0.081	+0.218	+0.189	+0.721	–0.362	+0.359
Me	+0.192	+0.117	+0.180	+0.157	+0.715	–0.362	+0.354
Et	+0.153	+0.076	+0.221	+0.197	+0.715	–0.361	+0.354
neo-Pent	+0.142	+0.075	+0.233	+0.201	+0.709	–0.360	+0.349
Ad	+0.087	+0.012	+0.300	+0.262	+0.704	–0.364	+0.340

Diadamantyl disulfide forms the most stable adduct with a very strong CT nature. As seen in Table 4, the partial charges in the organic groups are highest for the whole investigated series. At the same time, the formal charge of the nitrosonium ion goes from +1.000 to +0.340. The S–S bond length is predicted to be only 2.004 Å, and the C–S–S–C torsion angle increases from 109.0° to 141.2°. The di-*neo*-pentyl disulfide adduct also exhibits very strong CT leaving

Table 3. Calculated bond lengths [Å] and R–S–S–R torsion angle [°] for $[R_2S_2–NO]^+$ adducts and free R_2S_2 with selected organic substituents. Experimental bond parameters are shown where available.

R (a) $[R_2S_2–NO]^+$	CN	CF_3	4-Pyridyl[a]	H[b]	Ph[c]	2-Prop[d]	Me[e]	Et	*neo*-Pent	Ad
S1–S2	2.092	2.011	2.023	2.026	2.040	2.014	2.018	2.014	2.014	2.004
Calcd. exp.									2.0105(6)	
R1–S1	1.674	1.883	1.771	1.344	1.760	1.844	1797	1.822	1.827	1.869
Calcd. exp.									1.8121(6)	
R2–S2	1.673	1.870	1.773	1.342	1.775	1.842	1.802	1.825	1.827	1.870
Calcd. exp.									1.8226(5)	
S1–N	2.665	2.569	2.509	2.493	2.453	2.438	2.454	2.440	2.425	2.438
									2.3035(7)	
S2–O	3.020	2.978	2.950	2.857	2.934	2.916	2.876	2.882	2.907	2.903
									2.8592(7)	
N–O[f]	1.087	1.092	1.103	1.104	1.111	1.110	1.110	1.110	1.111	1.111
Calcd. exp.									1.1215(3)	
R1–S1–S2–R2	145.0	125.3	143.4	166.9	164.2	157.0	161.0	153.3	149.2	141.2
Calcd. exp.									160.20(2)	
ρ[g]	0.139	0.159	0.156	0.155	0.152	0.159	0.159	0.159	0.159	0.160
(b) R_2S_2										
S1–S2	2.071	2.013	2.020	2.043	2.017	2.021	2.030	2.030	2.028	2.033
Calcd. exp.			2.032(1)	2.0610(3)	2.0230(8)	2.0303(8)	2.03(1)			
R1–S1	1.680	1.840	1.772	1.343	1.781	1.847	1.809	1.827	1.838	1.858
Calcd. exp.			1.780(2)	1.3421(5)	1.7894(6)	1.830(2)	1.803(3)			
R2–S2	1.680	1.840	1.772	1.343	1.781	1.847	1.809	1.827	1.838	1.858
Calcd. exp.			1.7870(2)	1.3421(5)	1.7876(3)	1.838(5)	1.805(3)			
R1–S1–S2–R2	89.0	95.5	84.4	90.3	86.0	91.2	84.20	84.9	82.0	109.0
Calcd. exp.			84.0(1)	90.76(6)	84.99	89.0(1)	86.1(1)			
ρ[g]	0.143	0.157	0.156	0.149	0.156	0.155	0.153	0.153	0.153	0.151

[a] For experimental bond parameters, see ref.[21] [b] For experimental bond parameters, see ref.[22] [c] For experimental bond parameters, see ref.[23] [d] For experimental bond parameters, see ref.[24] [e] For experimental bond parameters, see ref. 21. [f] The computed N–O bond length of free NO^+ is 1.059 Å. [g] ρ is the electron density at the BCP of the S–S bond.

only a partial charge of +0.349 on the nitrosonium ion. In this case the organic group also adopts a high partial charge of +0.433. Like the diadamantyl disulfide adduct, the di-*neo*-pentyl disulfide adduct has a short S–S bond [calcd. 2.014; exp. 2.0105(6) Å]. The diethyl, dimethyl and di-2-propenyl disulfide adducts also show significant abilities for CT.

The diphenyl disulfide adduct is also predicted to be comparatively stable even though the phenyl group is electron-withdrawing and the S–S bond (2.040 Å) in the adduct is relatively long. The strong CT arises from the electron delocalization between the phenyl rings across the S–S bond. The nearly planar torsion angle (C–S–S–C) of 164.2° allows the formation of a conjugated bond structure, which significantly weakens the S–S bond, at the same time strengthening the S–C (1.760–1.775 Å) bonds. In the diphenyl disulfide adduct, the nitrosonium ion has a partial charge of only +0.345; just the diadamantyl disulfide adduct is predicted to have stronger CT. The large build up of positive charge renders the diphenyl disulfide adduct formation less favourable than adducts with electron-donating substituents on the sulfur atom. As with other electron-withdrawing groups, the competition for electron density between nitrosonium and the organic group results in a larger build up of positive charge on the sulfur atoms.

The hypothetical dicyano disulfide forms a very unstable adduct with the nitrosonium ion. Cyano groups withdraw electrons so strongly that, upon adduct formation, the S–S bond lengthens from 2.071 to 2.092 Å and the sulfur atoms carry very high partial positive charges (+0.658 and +0.633). The nitrosonium ion is also left with the highest positive charge of +0.626 in the series.

In summary, the ability of the organic substituents to accept positive charge stabilizes the disulfide adduct. Therefore, disulfides with electron-donating groups are expected to form relatively stable adducts with the nitrosonium ion. In some cases, the delocalization of electron density through conjugation may stabilize the disulfide nitrosonium adduct, as exemplified by the diphenyl disulfide–nitrosonium adduct. The adduct formation with disulfides containing electron-withdrawing organic substituents is generally not favourable as the CT is weak and the build up of positive charge at the sulfur atoms weakens the disulfide bond.

Orbital Analysis

The highest occupied molecular orbital (HOMO)–LUMO interaction of the CT complex formation of di-*neo*-pentyl disulfide adduct is illustrated in Figure 5. Electron density is transferred from the HOMO orbital of di-*neo*-pentyl disulfide, which is mainly a nonbonding orbital comprising of the free *p* electron pairs of the two sulfur atoms, to the antibonding LUMO orbital of the nitrosonium ion with a consequent shortening of the S–S bond and lengthening of the N–O bond. Natural bond orbital[25] (NBO) analysis indicates that electron density is transferred from the sulfur lone pairs to the nitrosonium antibonding orbitals. Adduct formation aligns the sulfur *p* orbitals towards the nitrosonium ion, which results in an increase in the R–S–S–R torsion angle.

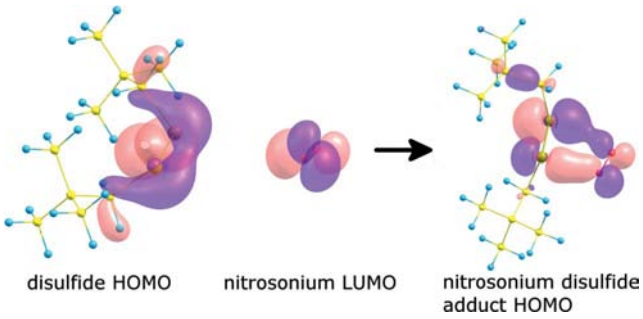

Figure 5. Interaction of the HOMO orbital of di-*neo*-pentyl disulfide and the LUMO orbital of the nitrosonium cation upon adduct formation.

The *p* lone pairs of the two sulfur atoms align towards the plane containing the nitrosonium LUMO orbital (π*) resulting in two new bonds: S1–N and S2–O. The HOMO of the adduct is bonding with respect to the S–N and S–O bonds, but antibonding with respect to the S–S and N–O bonds. The remaining sulfur lone pairs form a bonding π orbital with respect to the S–S bond. The antibonding effect of the HOMO orbital on the S–S bond is weaker than the bonding effect of the HOMO–1 orbital, as a larger part of the electron density of the HOMO orbital is donated to the nitrosonium LUMO orbital.

If a free diorgano disulfide is forced to adopt a C–S–S–C torsion angle of 180°, the HOMO orbital is fully antibonding with respect to the S–S bond, whereas the HOMO–1 is π bonding. This arrangement is unstable, but when the diorgano disulfide donates electron density from the HOMO orbital to the nitrosonium LUMO orbital, the π bonding overcomes the antibonding nature of the HOMO orbital. Therefore, the nearly planar sulfur framework becomes more stable.

In diorgano disulfide radical cations, C–S–S–C will adopt a fully planar orientation with a torsion angle of 180°. The highest singly occupied molecular orbital (SOMO) is antibonding with respect to the S–S bond and the two-electron HOMO–1 orbital is π bonding with respect to the S–S bond. This results in an approximate bond order of 1.5 for the S–S bond, which renders it stronger than the S–S bond in the neutral disulfide. The electron density of the S–S bond in dimethyl disulfide increases from 0.154 to 0.167 when one electron is removed. Therefore, the bond in the cation is shorter (1.993 Å) than that in the neutral dimethyl disulfide [calcd. 2.026; exp. 2.03(1) Å].[17] In the nitrosonium-bonded dimethyl disulfide complex the parameters are between the two extremes, the electron density value is 0.158 with bond length of 2.019 Å. Figure 6 shows a potential energy profile of Me_2S_2 and $Me_2S_2^+$ relative to the C–S–S–C torsion angle. The neutral disulfide prefers the dihedral angle near to 90° as a result of the minimized lone pair–lone pair interactions, whereas the cation adopts an angle of 180° to maximize π orbital overlap.

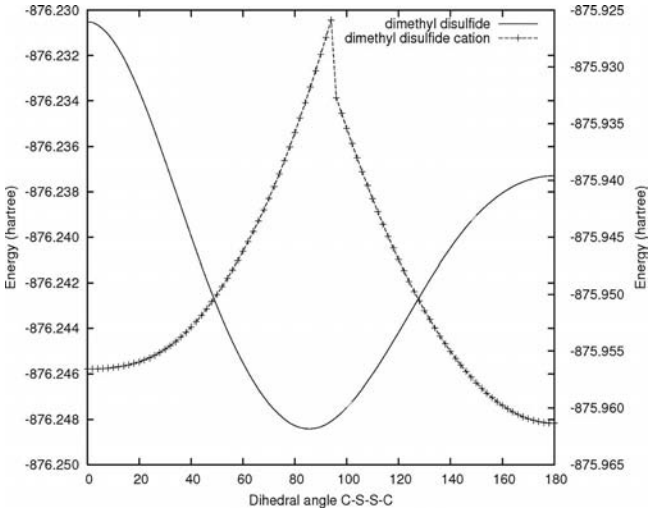

Figure 6. Potential energy profile of dimethyl disulfide and its cation as a function of the C–S–S–C torsion angle.

Figure 7 illustrates the HOMO–1 π orbital and the HOMO orbital of dimethyl disulfide when the C–S–S–C torsion angle is 180°. The cationic dimethyl disulfide has very similar orbital structure (not shown). The main difference is that the HOMO orbital is split into a SOMO and a LUMO.

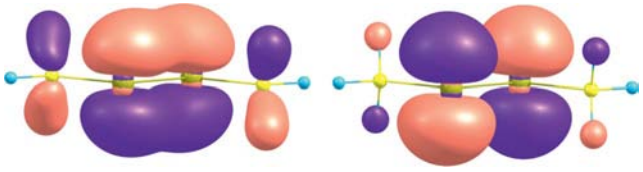

Figure 7. The HOMO–1 orbital (left), and the HOMO orbital (right) in dimethyl disulfide.

Conclusions

We have presented three new diorgano dichalcogenide adducts, two of which are CT adducts of dimethyl diselenide and diiodine with different stoichiometries. $[Me_2Se_2{\cdot}I_2]$ and $[Me_2Se_2{\cdot}2I_2]$ complete the series of possible diorgano diselenide–diiodine adducts with simple stoichiometries (2:1, 1:1, 1:2) together with $[(TIP_2Se_2)_2{\cdot}I_2]$[11] and $[Ph_2Se_2{\cdot}I_2]$.[12] The adduct $[C_{10}H_{22}S_2{\cdot}NO^+TfO^-]$ can be used as an example of the uncompleted redox process in nitrosation reactions[10] as well as a hint for the coordination of NO and its derivatives in biochemistry.[5–8]

The main mechanism behind the CT adduct formation is electron transfer from the sulfur *p* lone pairs to the nitrosonium N–O antibonding orbital. CT, S–S π-orbital formation and the mutually lowered repulsion from sulfur lone pairs contribute to the adduct stability. Strong electron-donating groups stabilize the adducts by preventing the build up of charge on the sulfur atoms. Similarly, electron-withdrawing substituents, which can conjugate the electron density across the S–S bond, can also stabilize the adduct as indicated by the hypothetical diphenyl disulfide adduct.

Experimental Section

General: All reactions were carried out under dry argon. Dry solvents (standard methods) were used throughout. Elemental analyses are missing due the fact that the adducts are sensitive to hydrolysis and/or not stable at room temperature.

Syntheses

$[Me_2Se_2{\cdot}2I_2]$: NO^+TfO^- (0.36 g, 2.01 mmol) dissolved in C_2H_5CN (1 mL) was added to a suspension of Me_2Se_2 (0.26 g, 1.38 mmol) and I_2 (0.51 g, 2.01 mmol) in C_2H_5CN (5 mL) at –25 °C. After precipitation and washing with Et_2O, the main product, $[(MeSe)_4^{2+}(TfO^-)_2]$,[14] was obtained as an orange precipitate (0.19 g, 20%) with a minor black product. Crystals suitable for crystal structure determination were grown from a mixture of C_2H_5CN and *N*,*N*-dimethylformamide (DMF, 2:1).

$[Me_2Se_2{\cdot}I_2]$. Method 1: I_2 (0.16 g, 0.63 mmol) was dissolved in pentane and Me_2Se_2 (0.19 g, 1.01 mmol) was added into a solution of NO^+TfO^- (0.45 g, 2.51 mmol) dissolved in C_2H_5CN (5 mL) at –25 °C. The two phases were stirred intensely for 30 min. The pentane phase was removed, and the C_2H_5CN phase was evaporated. The glittering orange precipitate (0.31 g, 70%) was dried and redissolved in C_2H_5CN. Cooling to –80 °C yielded red-black crystals. **Method 2:** Me_2Se_2 (0.38 g, 2.02 mmol) was added to a suspension of I_2 (0.51 g, 2.01 mmol) in C_2H_5CN (5 mL) at –80 °C. The resulting suspension was stirred at room temp. until all I_2 had dissolved. Upon cooling the reaction mixture to –80 °C some unreacted I_2 precipitated. The main product was obtained as brown-red crystals (0.75 g, 85%). $^{13}C\{^1H\}$ NMR (DMF/CD_3CN): δ = 18.6, 14.5 ppm. $^{77}Se\{^1H\}$ NMR (DMF/CD_3CN): δ = 423 ppm.

Diethyl Ditelluride, Diiodine and Nitrosyl Triflate: NO^+TfO^- (0.43 g, 2.40 mmol) dissolved in CH_3CN (1 mL) was added to a suspension of Et_2Te_2 (0.38 g, 1.21 mmol) and I_2 (0.31 g, 1.22 mmol) in CH_3CN (5 mL) at –30 °C. After reducing the amount of red solution by evaporation and washing with Et_2O, a black precipitate of $[(EtTe)_4^{2+}(TfO^-)_2]$[14] together with unreacted I_2 was obtained.

Dimethyl Disulfide and Nitrosyl Triflate: Me_2S_2 (0.38 g, 4.03 mmol) was added to a solution of NO^+TfO^- (0.72 g, 4.02 mmol) in CH_3CN (15 mL) at –25 °C. The colourless solution immediately turned dark red. After evaporating the solvent, a green-blue oil was obtained.

Diethyl Disulfide and Nitrosyl Triflate: Et_2S_2 (0.37 g, 3.03 mmol) was added to a solution of NO^+TfO^- (0.54 g, 3.02 mmol) in C_2H_5CN (7 mL) at –25 °C. The colourless solution immediately turned yellow-brown. Upon cooling to –80 °C, yellow needles were observed, but they were only stable for minutes and X-ray crystallography was not possible.

$[C_{10}H_{22}S_2{\cdot}NO^+TfO^-]$: *neo*-$Pent_2S_2$ (0.62 g, 3.00 mmol) was added to a solution of NO^+TfO^- (0.54 g, 3.02 mmol) in C_2H_5CN (5 mL) at –25 °C. The colourless solution immediately turned red. After reducing the solvent to ca. 1 mL and cooling to –80 °C, the adduct was quantitatively obtained as green crystals (Table 5).

X-ray Crystallography

Analytically pure samples were obtained by crystallization from the solvents mentioned above. With a special apparatus,[26] suitable crystals were mounted and measured with a Bruker Smart CCD 1000 diffractometer (Mo-K_α radiation, graphite monochromator) under cooling and an inert gas atmosphere. After a semiempirical absorption correction by equalizing symmetry-equivalent reflections (SADABS), structure solution and refinement were carried out with the SHELX programs.[27] Illustration of the crystal structures was performed with Diamond 3.1.[28]

Table 5. Crystal and structure refinement data for $[Me_2Se_2{\cdot}2I_2]$, $[Me_2Se_2{\cdot}I_2]$ and $[C_{10}H_{22}S_2{\cdot}NO^+TfO^-]$.

	$[Me_2Se_2{\cdot}2I_2]$	$[Me_2Se_2{\cdot}I_2]$	$[C_{10}H_{22}S_2{\cdot}NO^+TfO^-]$
Empirical formula	$C_2H_6Se_2I_4$	$C_2H_6Se_2I_2$	$C_{11}H_{22}O_4F_3S_3N$
Formula weight [g/mol]	695.61	441.79	385.48
Crystal size	0.5, 0.15, 0.1	0.3, 0.1, 0.05	0.5, 0.5, 0.1
Crystal colour	black needle	red-black needle	green prism
Space group	$P2_1/n$	$P2_1/n$	$C2/c$
a [Å]	6.5260(10)	9.675(2)	27.469(10)
b [Å]	8.5911(14)	5.8376(16)	8.375(3)
c [Å]	11.155(3)	15.304(3)	16.151(6)
β [°]	103.84(3)	98.420(16)	106.749(7)
V [Å^3]	607.2(2)	855.0(4)	3558(2)
Z	2	4	8
$D_{calcd.}$ [g cm^{-3}]	3.804	3.432	1.439
μ [mm^{-1}]	16,194	15.769	0.459
Temperature [K]	133(2)	133(2)	133(2)
$T_{min.}$, $T_{max.}$	0.508, 1.000	0.439, 1.000	0.439, 1.000
Measured reflections	1856	2536	2165
Independent reflections	1581	1658	1334
R_1/wR_2 [$I > 2(I)$]	0.0192, 0.0436	0.0456, 0.0992	0.0691, 0.1580
R_1/wR_2 (all reflections)	0.0250, 0.0458	0.0829, 0.1116	0.1198, 0.2131
S	1.041	1.084	1.035
Refined parameters	40	58	206
Residual electron density [e Å^{-3}], between:	–0.765 and 1.779	–1.555 and 2.301	–0.472 and 0.857

CCDC-828788 (for $[Me_2Se_2{\cdot}2I_2]$), -828787 (for $[Me_2Se_2{\cdot}I_2]$) and -828789 (for $[C_{10}H_{22}S_2{\cdot}NO^+TfO^-]$) contain the supplementary crystallographic data for this paper. These data can be obtained free of charge from The Cambridge Crystallographic Data Centre via www.ccdc.cam.ac.uk/data_request/cif.

All computations were performed using localized density functional theory M06L[29] involving def2-TZVPP[30] basis sets. Computations were performed with Gaussian09[31] quantum chemical program package. Atoms in molecules (AIM) electron density was computed with the AIMAll[32] program. NBO analysis was performed with the NBO[25] program. BSSE error was estimated to be less than 2 kJ/mol and thus no BSSE corrections were deemed necessary. All given energies are standard Gibbs energies calculated at 298.15 K and 101.325 kPa. All structures are at local minima in their respective potential energy surfaces.

The MO analysis is based on structures optimized in the gaseous phase. The relaxed potential energy surface scan shown in Figure 6 was computed in the gaseous phase. The computed standard Gibbs energies, AIM charges and structural parameters presented in Table 3 and Table 4 are based on structures optimized with an implicit solvation model (CPCM,[33] acetonitrile).

Acknowledgments

We thank the Fonds der Chemischen Industrie, the Deutsche Forschungsgemeinschaft (DFG), the Academy of Finland and the Inorganic Materials Chemistry Graduate Program supported by the Finnish Ministry of Education (to T. T. T) for support of this work. We are also grateful to the Finnish CSC – IT Center for Science for allocation of computational resources.

[1] a) F. A. Devillanova, *Handbook of Chalcogen Chemistry – New Perspectives in Sulfur, Selenium and Tellurium*, RSC Publishing, Cambridge, **2007**; b) M. C. Aragoni, M. Arca, F. A. Devillanova, P. Grimaldi, F. Isaia, F. Lelj, V. Lippolis, *Eur. J. Inorg. Chem.* **2006**, 2166; c) W. T. Pennington, T. W. Hanks, H. D. Arman, *Struct. Bonding (Berlin)* **2008**, *126*, 65.

[2] a) C. Raby, J. Buxeraud, *Eur. J. Med. Chem.* **1980**, *15*, 425; b) J. Buxeraud, A.-C. Absil, J. Claude, C. Raby, G. Catanzano, C. Beck, *Eur. J. Med. Chem.* **1985**, *20*,43; c) M. H. Hussian, E. J. Lien, *J. Med. Chem.* **1971**, *14*, 138; d) L. Jirousek, M. Soodak, *J. Pharmacol. Exp. Ther.* **1974**, *191*, 341; e) K. Hofmann, in: *The Chemistry of Heterocyclic Compounds* (Ed.: A. Weissberger), Interscience, London, **1953**; f) L. S. Goodman, A. Gilman, *The Pharmacological Basis of Therapeutics*, 5th ed., Macmillan, New York, **1975**; g) C. Raby, J.-F. Lagorce, A.-C. Jambut-absil, J. Buxeraud, G. Catanzano, *Endocrinology* **1990**, *126*, 1683; h) A.-C. Jambut-Absil, J. Bauxeraud, C. Moesch, J.-F. Lagorce, C. Raby, *Heterocycles* **1986**, *24*, 1995; i) L. Liu, W. A. Baase, B. W. Matthews, *J. Mol. Biol.* **2009**, *385*, 595; j) G. Roy, K. P. Bhabak, G. Mugesh, *Cryst. Growth Des.* **2011**, *11*, 2279; k) C. D. Antoniadis, S. K. Hadjikakou, N. Hadjiliadis, A. Papakyriakou, M. Baril, I. S. Butler, *Chem. Eur. J.* **2006**, *12*, 6888.

[3] J. R. Ferraro, J. M. Williams, *Introduction to Synthetic Electrical Conductors*, Academic Press, New York, **1987**.

[4] M. C. Aragoni, M. Arca, F. A. Devillanova, A. Garau, F. Isaia, V. Lippolis, G. Verani, *Coord. Chem. Rev.* **1999**, *184*, 271.

[5] a) D. L. H. Williams, *Nitrosation*, Cambridge University Press, Cambridge, **1988**; b) P. P. Kadzyauskas, N. S. Zefirov, *Usp. Khim.* **1968**, *37*, 1243 [*Russ. Chem. Rev.* **1968**, *37*, 543]; c) P. B. D. De la Mare, R. Bolton, *Electrophilic Additions to Unsaturated Systems*, Amsterdam, Elsevier, **1982**; d) L. F. Fieser, M. Fieser, *Reagents for Organic Synthesis*, New York, Wiley, **1968**; e) G. A. Olah, K. K. Laali, Q. Wang, G. K. S. Prakash, *Onium Ions*, John Wiley & Sons, New York, **1998**.

[6] a) E. Culotta, D. E. Koshland, *Science* **1992**, *258*, 1862; b) A. R. Butler, D. L. H. Williams, *Chem. Soc. Rev.* **1993**, *22*, 233; c) M. Fontecave, J.-L. Pierre, *Bull. Soc. Cim. Fr.* **1994**, *131*, 620; d) A. R. Butler, *Chem. Ind.* **1995**, 828; e) J. S. Stamler, M. Feelisch, *Methods in Nitric Oxide Research*, Chichester, Wiley, **1996**; f) F. Murad, *Angew. Chem.* **1999**, *111*, 1976; *Angew. Chem. Int. Ed.* **1999**, *38*, 1856; g) R. F. Furchgott, *Angew. Chem.* **1999**, *111*, 1990; *Angew. Chem. Int. Ed.* **1999**, *38*, 1870; h) L. J. Ignarro, *Angew. Chem.* **1999**, *111*, 2002; *Angew. Chem. Int. Ed.* **1999**, *38*, 1882; i) R. P. Patel, J. McAndrew, H. Sellak, C. R. White, H. Jo, B. A. Freeman, V. M. Darley-Usmar, *Biochim. Biophys. Acta Bioenerg.* **1999**, *1411*, 385.

[7] a) S. A. Lipton, Y.-B. Choi, Z.-H. Pan, S. Z. Lei, H.-S. V. Chen, N. J. Sucher, J. Loscalzo, D. J. Singel, J. S. Stamler, *Nature*

(London) **1993**, *364*, 626; b) J. S. Stamler, D. J. Singel, J. Loscalzo, *Science* **1992**, *258*, 1898; c) A. R. Butler, F. W. Flitney, D. L. H. Williams, *Trends Pharmacol. Sci.* **1995**, *16*, 18; d) M. A. De Groote, T. Testerman, Y. Xu, G. Stauffer, F. C. Fang, *Science* **1996**, *272*, 414; e) M. N. Hughes, *Biochim. Biophys. Acta Bioenerg.* **1999**, *1411*, 263; f) S. Y. Shaban, R. van Eldik, *Dalton Trans.* **2011**, *40*, 287; g) T. C. Harrop, D. Song, S. J. Lippard, *J. Inorg. Biochem.* **2007**, *101*, 1730.

[8] a) J. J. Kirchner, S. T. Sigurdsson, P. B. Hopkins, *J. Am. Chem. Soc.* **1992**, *114*, 4021; b) A. H. Elcock, P. D. Lyne, A. J. Mulholland, A. Nandra, W. G. Richards, *J. Am. Chem. Soc.* **1995**, *117*, 4706.

[9] a) P. Mack, J. M. Dyke, T. G. Wright, *Chem. Phys.* **1997**, *218*, 243; b) L. Angel, A. J. Stace, *J. Phys. Chem. A* **1998**, *102*, 3037.

[10] G. I. Borodkin, V. G. Shubin, *Russ. Chem. Rev.* **2001**, *70*, 211.

[11] W.-W. du Mont, A. Martens, S. Pohl, W. Saak, *Inorg. Chem.* **1990**, *29*, 4848.

[12] S. Kubiniok, W.-W. du Mont, S. Pohl, W. Saak, *Angew. Chem.* **1988**, *100*, 434; *Angew. Chem. Int. Ed. Engl.* **1988**, *27*, 431.

[13] a) N. A. Barnes, S. M. Godfrey, R. T. A. Halton, I. Mushtaq, R. G. Pritchard, *Dalton Trans.* **2008**, 1346; b) C. G. Hrib, P. G. Jones, W.-W. du Mont, V. Lippolis, F. A. Devillanova, *Eur. J. Inorg. Chem.* **2006**, 1294; c) W.-W. du Mont, M. Bätcher, C. Daniliuc, F. A. Devillanova, C. Druckenbrodt, J. Jeske, P. G. Jones, V. Lippolis, F. Ruthe, E. Seppälä, *Eur. J. Inorg. Chem.* **2008**, 4562.

[14] B. Müller, H. Poleschner, K. Seppelt, *Dalton Trans.* **2008**, *33*, 4424.

[15] A. Bondi, *J. Phys. Chem.* **1964**, *68*, 441.

[16] a) N. A. Barnes, P. Bhattacharyya, S. M. Godfrey, R. T. A. Halton, I. Mushtaq, R. G. Pritchard, *Phosphorus Sulfur Silicon Relat. Elem.* **2005**, *180*, 783; b) P. D. Boyle, S. M. Godfrey, *Coord. Chem. Rev.* **2001**, *223*, 265.

[17] O. Mundt, G. Becker, J. Baumgarten, H. Riffel, A. Simon, *Z. Anorg. Allg. Chem.* **2006**, *632*, 1687.

[18] R. Minkwitz, G. Nowicki, *Inorg. Chem.* **1991**, *30*, 4426.

[19] a) M. L. Golden, J. C. Yarbrough, J. H. Reibenspies, M. Y. Darensbourg, *Inorg. Chem.* **2004**, *43*, 4702; b) T. Gunnlaugsson, P. E. Kruger, P. Jensen, F. M. Pfeffer, G. M. Hussey, *Tetrahedron Lett.* **2003**, *44*, 8909; c) H. M. Brownlee, S. Schreiner, Abstracts of Papers, *227th ACS National Meeting*, Anaheim, CA, United States, March 28 – April 1, **2004**, CHED-456; d) B. Botta, I. D'Acquarica, G. Delle Monache, L. Nevola, D. Tullo, F. Ugozzoli, M. Pierini, *J. Am. Chem. Soc.* **2007**, *129*, 11202.

[20] S. V. Rosokha, S. V. Lindemann, R. Rathore, J. K. Kochi, *J. Org. Chem.* **2003**, *68*, 3947.

[21] F. M. Tabellion, S. R. Seidel, A. M. Arif, P. J. Stang, *J. Am. Chem. Soc.* **2001**, *123*, 7740.

[22] C. J. Marsden, B. J. Smith, *J. Phys. Chem.* **1988**, *92*, 347.

[23] M. Sacerdoti, G. Gilli, P. Domiano, *Acta Crystallogr., Sect. B* **1975**, *31*, 327.

[24] B. Bartkowska, C. Kruger, *Acta Crystallogr., Sect. C* **1997**, *53*, 1064.

[25] NBO 5.0, E. D. Glendening, J. K. Badenhoop, A. E. Reed, J. E. Carpenter, J. A. Bohmann, C. M. Morales, F. Weinhold, Theoretical Chemistry Institute, University of Wisconsin, Madison, WI; http://www.chem.wisc.edu/~nbo5, **2001**.

[26] H. Schumann, W. Genthe, E. Hahn, M.-B. Hossein, D. van der Helm, *J. Organomet. Chem.* **1986**, *28*, 2561.

[27] a) G. Sheldrick, *Program for Crystal Structure Solution*, Göttingen, **1986**; b) G. Sheldrick, *SHELXS-93*, Göttingen, **1993**.

[28] K. Brandenburg, *Diamond*, version 3.1, Crystal Impact GbR, **1996**.

[29] Y. Zhao, D. G. Truhlar, *J. Chem. Phys.* **2006**, *125*, 194101.

[30] A. Schäfer, C. Huber, R. Ahlrichs, *J. Chem. Phys.* **1994**, *100*, 5829.

[31] M. J. Frisch, G. W. Trucks, H. B. Schlegel, G. E. Scuseria, M. A. Robb, J. R. Cheeseman, G. Scalmani, V. Barone, B. Mennucci, G. A. Petersson, H. Nakatsuji, M. Caricato, X. Li, H. P. Hratchian, A. F. Izmaylov, J. Bloino, G. Zheng, J. L. Sonnenberg, M. Hada, M. Ehara, K. Toyota, R. Fukuda, J. Hasegawa, M. Ishida, T. Nakajima, Y. Honda, O. Kitao, H. Nakai, T. Vreven, J. A. Montgomery Jr, J. E. Peralta, F. Ogliaro, M. Bearpark, J. J. Heyd, E. Brothers, K. N. Kudin, V. N. Staroverov, R. Kobayashi, J. Normand, K. Raghavachari, A. Rendell, J. C. Burant, S. S. Iyengar, J. Tomasi, M. Cossi, N. Rega, J. M. Millam, M. Klene, J. E. Knox, J. B. Cross, V. Bakken, C. Adamo, J. Jaramillo, R. Gomperts, R. E. Stratmann, O. Yazyev, A. J. Austin, R. Cammi, C. Pomelli, J. W. Ochterski, R. L. Martin, K. Morokuma, V. G. Zakrzewski, G. A. Voth, P. Salvador, J. J. Dannenberg, S. Dapprich, A. D. Daniels, Ö. Farkas, J. B. Foresman, J. V. Ortiz, J. Cioslowski, D. J. Fox, *Gaussian 09*, revision B.01, Gaussian, Inc., Wallingford CT, **2009**.

[32] Todd A. Keith, *AIMAll*, version 11.03.14, **2011** (aim.tkgristmill.com).

[33] M. Cossi, N. Rega, G. Scalmani, V. Barone, *J. Comput. Chem.* **2003**, *24*, 669.

Received: June 20, 2011
Published Online: September 27, 2011

